Species Differences in Response to Binding Interactions of Bisphenol A and its Analogs with the Modeled Estrogen Receptor 1 and In Vitro Reporter Gene Assay in Human and Zebrafish

Park, Chang Gyun; Singh, Nancy; Ryu, Chang Seon; Yoon, Ju Yong; Esterhuizen, Maranda ...

2022-10
Oxford University Press
http://hdl.handle.net/10138/563497
Park, C G, Singh, N, Ryu, C S, Yoon, J Y, Esterhuizen, M & Kim, Y J 2022, 'Species Differences in Response to Binding Interactions of Bisphenol A and its Analogs with the Modeled Estrogen Receptor 1 and In Vitro Reporter Gene Assay in Human and Zebrafish', Environmental Toxicology and Chemistry, vol. 41, no. 10, pp. 2431–2443. https://doi.org/10.1002/etc.5433

Species Differences in Response to Binding Interactions of BPA and its Analogs with the Modeled Estrogen Receptor 1 and *In Vitro* Reporter Gene Assay in Human and Zebrafish

Chang Gyun Park,[1,2] Nancy Singh,[1,2] Chang Seon Ryu,[1] Ju Yong Yoon,[1] Maranda Esterhuizen,[1,3] and Young Jun Kim[1]*

[1] Environmental Safety Group, Korea Institute of Science and Technology (KIST) Europe, Saarbrucken 66123, Germany

[2] Universität des Saarlandes, 66123 Saarbrücken, Germany

[3] University of Helsinki, Ecosystems and Environment Research Programme, Faculty of Biological and Environmental Sciences, Niemenkatu 73, 15140 Lahti, Finland and Helsinki Institute of Sustainability Science (HELSUS), Fabianinkatu 33, 00014 Helsinki, Finland

***Correspondence** Young Jun Kim, Environmental Safety Group, Korea Institute of Science and Technology (KIST) Europe, Campus E.71, Saarbruecken, Saarland 66123 Germany. Tel.: +49-681-9382-327; Fax: +49-681-9382-319; Email: youngjunkim@kist-europe.de

3/31/22; 5/12/22; 7/12/22

Abstract: Adverse impacts associated with the interactions of numerous endocrine-disruptor chemicals (EDCs) with estrogen receptor 1 play a pivotal role in reproductive dysfunction. The predictive studies on these interactions thus are crucial in the risk assessment of EDCs but heavily rely on the accuracy of specific protein

This article has been accepted for publication and undergone full peer review but has not been through the copyediting, typesetting, pagination and proofreading process, which may lead to differences between this version and the Version of Record. Please cite this article as doi: 10.1002/etc.5433.

structure in 3D. As the three-dimensional (3D) structure of zebrafish estrogen receptor 1 (zEsr1) is not available, the 3D structure of zEsr1 ligand-binding domain (zEsr1-LBD) was generated using MODELLER, and its quality was assessed by PROCHECK, ERRAT, ProSA, and Verify-3D tools. After the generated model was verified as reliable, bisphenol A (BPA) and its analogs were docked on the zEsr1-LBD and human estrogen receptor 1 ligand-binding domain (hESR1-LBD) using Discovery Studio and Autodock Vina programs. Besides, molecular dynamics followed by molecular docking were simulated using the NAMD program and compared to those of the *in vitro* reporter gene assays. Some chemicals were bound with an orientation similar to that of 17β-estradiol (E2) in both models and *in silico* binding energies showed moderate or high correlations with *in vitro* results ($0.33 \leq r^2 \leq 0.71$). Notably, hydrogen bond occupancy during molecular dynamics simulations exhibited a high correlation with *in vitro* results ($r^2 \geq 0.81$) in both complexes. These results showed that the combined *in silico* and *in vitro* approaches can be provided the valuable tools for identifying EDCs in different species, facilitating the assessment of EDC-induced reproductive toxicity.

Keywords: *In silico* methods; Homology modeling; Estrogen receptor 1; Zebrafish; BPA and its analogs; *In vitro* assay

This article includes online-only Supporting Information.

*Address correspondence to youngjunkim@kist-europe.de

Published online XXXX 2022 in Wiley Online Library (www.wileyonlinelibrary.com).

DOI: 10.1002/etc.xxxx

Introduction

Estrogen-induced actions promote various physiological processes, such as growth, homeostasis, and reproduction (Barkhem et al., 2004; Kovats, 2015; Shen and

Shi, 2015; Hewitt et al., 2016; Khalid and Krum, 2016). Additionally, estrogens regulate pubertal development and function of the female reproductive system (Hewitt et al., 2016), bone density (Khalid and Krum, 2016), immune system (Kovats, 2015), and lipid and glucose metabolism (Shen and Shi, 2015). Most of these processes are mediated by estrogen receptors (ESRs), which can be divided into two subtypes: estrogen receptor 1 (ESR1) and estrogen receptor 2 (ESR2). Both receptors have been observed in non-mammalian vertebrates and mammals (Hawkins et al., 2000). ESR1 is predominantly expressed in various tissues and organs, such as the liver, bones, glands, uterus, ovaries, testes, and prostate (Dahlman-Wright et al., 2006; Heldring et al., 2007), and plays more important roles than ESR2 in the mammary glands and uterus, maintenance of skeletal homeostasis, and regulation of lipid and glucose metabolism (Barros and Gustafsson, 2011; Paterni et al., 2014). ESRs are structurally composed of N-terminal, DNA-binding, and ligand-binding domains (Kumar et al., 2011). The LBD includes the ligand-binding pocket, which can activate ESRs by interacting with ligands, such as 17β-estradiol (E2). Owing to this interaction, many exogenous chemicals, which mimic estrogens, can alter the functions of the endocrine system and cause various adverse effects (Bardet et al., 2002). Therefore, concern regarding the possible threats posed by endocrine-disrupting chemicals (EDCs) in wildlife and humans is increasing (Mills and Chichester, 2005; Zhang and Zhou, 2005).

Bisphenol A (BPA) has been reported to adversely affect the reproductive and developmental systems of humans, fish, and amphibians (Kang et al., 2007; Rochester, 2013; Mathieu-Denoncourt et al., 2015), and is a precursor to plastics, epoxy resins, and thermal paper (Geens et al., 2012). Although substitutes have recently been manufactured to replace BPA, some exert endocrine effects similar to those of BPA (Rosenmai et al., 2014; Chen et al., 2016; Usman and Ahmad, 2016; Keminer et al.,

2020). As a large number of comprehensive studies are required to evaluate potential endocrine disruption caused by BPA substitutes, molecular docking is a promising tool for predicting and screening potential EDCs, and has been conducted to predict the types of interactions, binding affinity, and orientations of the docked ligands at the binding site of the target receptor (Babu et al., 2012; Montes-Grajales and Olivero-Verbel, 2013; Sliwoski et al., 2013; Cavaliere et al., 2020). However, since most static docking protocols lack receptor flexibility, the reliability of the complexes might be uncertain (Kale et al., 1999). Hence, molecular dynamics (MD) simulation has been applied to understand the dynamic behavior of complexation and provide significant complementary with molecular docking. MD simulation can offer fundamental molecular mechanisms and conformational changes (Kale et al., 1999; Phillips et al., 2005). Although most docking studies have been conducted on BPA and its analogs for human ESRs, docking and MD simulations for aquatic organisms remain limited as there are currently no available crystal structures (Babu et al., 2012; Zhang et al., 2018).

Therefore, this study aimed to generate the structure of a zEsr1-LBD using homology modeling. Zebrafish (*Danio rerio*) have been utilized as a model organism for toxicity testing by the Organization for Economic Co-operation and Development (OECD) guidelines. Furthermore, zebrafish exhibit rapid development and growth, and signaling pathways highly similar to those in humans (Kari et al., 2007; MacRae and Peterson, 2015). The zEsr1-LBD was generated using the MODELLER program and the structural quality was then verified using PROCHECK, ERRAT, ProSA, and Verify-3D tools. Consequently, the generated zEsr1-LBD model was used to investigate its interactions with E2, BPA, 4,4′-(9-Fluorenyliden)-diphenol (BPFL), tetramethyl bisphenol A (TMBPA), and 4-phenylphenol. BPFL, TMBPA, and 4-phenylphenol are classified as alternative substances of BPA, and these analogs are

introduced mainly for the usage in thermal paper, polymer, polycarbonate, and fire retardant (Keminer et al., 2020). As these applications cause exposure of chemicals into the environment, the analogs have been detected in nature with environmental relevance (Jin and Zhu, 2016; Banaderakhshan et al., 2022; Chafi et al., 2022). These chemicals have been reported to have endocrine disruptor potential by exhibiting anti- or estrogenic activities in humans (Keminer et al., 2020). In addition, BPFL showed anti-estrogenic effect in mice and zebrafish and hormetic effects on regulating hypothalamic-pituitary-thyroid axis in zebrafish (Zhang et al., 2017; Mi et al., 2019; Jin et al., 2021). However, there is still a lack of studies on their estrogenic disruptive activities and their modes of action in aquatic species. Thereby, the complex geometry and putative chemical-receptor binding energies of BPA and its analogs were then calculated and validated by conducting *in vitro* assays. The correlations between the *in silico* and *in vitro* analyses confirmed that the newly generated zEsr1-LBD is useful for predicting and evaluating the estrogenic activities of EDCs.

Materials and methods

Sequence alignment, template selection, and homology modeling

Sequence alignment was conducted to observe sequence identity between human ESRs (hESRs) and zebrafish Esrs (zEsrs). Multiple sequence alignment and Principal Components Analysis (PCA) were conducted, and a phylogenetic tree was generated using JalView (Procter et al., 2021). The PCA and phylogenetic tree were constructed using amino acid sequences of estrogen receptors available from Uniprot. The sequence sources and UniProt IDs were as follows: human estrogen receptor 1 (hESR1, P03372), zebrafish estrogen receptor 1 (zEsr1, P57717), human estrogen receptor 2 (hESR2, Q92731), zebrafish estrogen receptor 2a (zEsr2a, Q7ZU32), and zebrafish estrogen receptor 2b (zEsr2b, Q90WS9).

The crystal structure of hESR1 (PDB ID: 2YJA) was selected as hESR1-LBD, which is bounds to stapled peptides and E2 (Phillips et al., 2011). The LBD structure of zEsr1 was created using homology modeling. First, the LBD sequence of zEsr1 (P57717) was retrieved from the UniProt database to build the model. The query sequence was then used to search for an optimal template with the protein-basic local alignment search tool (BLASTp) (Altschul et al., 1990). hESR1-LBD (2YJA) was selected as the optimal template after utilizing BLASTp. MODELLER 9.25 was used to create the homology model for zEsr1-LBD. The program is a homology or comparative modeling tool that conducts comparative protein structure modeling based on satisfaction of spatial restraints. Comparative modeling predicts the 3D structure of a given protein target sequence based primarily on its alignment with one or more proteins with known template structures to generate a zebrafish Esr1 model (Webb and Sali, 2016). The LBD sequence of zEsr1 and template structure (2YJA) were used as the inputs in MODELLER v9.25 (https://salilab.org/modeller/9.25/release.html). When target-template alignment is conducted, the program automatically calculates a 3D model of the target using its automodel class (Webb and Sali, 2016). MODELLER finally generates a 3D model containing all the main chain and sidechain non-hydrogen atoms as the output of the given target sequence. Ten models were generated, and one structure with the lowest DOPE score was selected as the zEsr1-LBD model for molecular docking (Shen and Sali, 2006).

Homology model validation

The structural qualities of zEsr1-LBD and hESR1-LBD were validated using ERRAT (Colovos and Yeates, 1993), PROCHECK (Morris et al., 1992), ProSA (Wiederstein and Sippl, 2007), and Verify 3D tools (Lüthy et al., 1992). ERRAT analyzes the relative frequencies of non-covalent interactions between various types

of atoms (Colovos and Yeates, 1993), while PROCHECK uses the Ramachandran plot for structural verification, which assesses the quality and accuracy of the stereochemical properties of a model (Morris et al., 1992). The Protein Structure Analysis (ProSA) program is an established tool with a large user base that is frequently used to refine and validate experimental protein structures and for structural prediction and modeling (Wiederstein and Sippl, 2007). The program Verify 3D measures the compatibility of a protein model with its own amino acid sequence (Lüthy et al., 1992).

Molecular Docking

The hESR1-LBD and generated zEsr1-LBD structures were used for molecular docking with BPA analogues including E2, BPA, BPFL, TMBPA, and 4-phenylphenol as the test ligands from the PubChem database (E2: 5757, BPA: 6623, BPFL: 76716, TMBPA: 79717, and 4-phenylphenol: 7103). All the chemicals were saved as a SDF file, and their geometries were optimized following the MM2 energy minimization method. The files were converted into PDB format using Discovery Studio Visualizer 2016 (Accelrys Software Inc., San Diego, CA, USA).

Molecular docking simulations were conducted using the CDOCKER module of Discovery Studio (Wu et al., 2003) and AutoDock Vina (Trott and Olson, 2010), which uses the CHARMM-based molecular dynamics method. CDOCKER generates the conformation using high-temperature MD and then forwarding the conformations to the binding site for binding pose analysis. The CDOCKER interaction energy is taken as an estimate of the molecular binding affinity, with lower values suggesting more favorable binding between the protein and ligand (Wu et al., 2003). Autodock Vina utilizes protein and ligand information, along with the grid box properties, in the docking configuration file, and assumes that the receptor is rigid and ligands are flexible during docking (Trott and Olson, 2010). Root-mean-squared-deviation

(RMSD) values below 1.0 Å were clustered and considered the results with the most favorable binding free energy. The grid size was set to 40 points each in the x, y, and z directions, with a grid spacing of 1.0 Å. The energetic map was determined using the distance-dependent function of the dielectric constant, and the default settings were applied to all the other parameters. All docked poses were determined using rankings based on binding energies. The pose with the lowest binding energy was extracted and aligned with the receptor structure for further analysis.

Molecular dynamics (MD) simulations

All simulations were performed using the nanoscale molecular dynamics (NAMD) 2.14 software with the CHARMM27 force field (Phillips et al., 2005). System preparations for MD simulations and analysis of the computed trajectories were performed using visual dynamics studio (VMD) v1.9 (Humphrey et al., 1996). The CHARMM GUI web server was utilized to prepare the system for the MD simulations, including ligand parameter files. Coordinates for the missing hydrogen atoms and amino acids side chains were added with AutoPSF plugin from VMD and based on the CHARMM27 force field (Kalé et al., 1999). The system was solvated with TIP3P water using the solvate plugin from VMD with a spacing of 10 Å in all directions (Jorgensen et al., 1983). The MD simulations were considered Na^+ and Cl^- ions in explicit water for neutralizing the charges of the system. After the minimization of the solvated system, the system was equilibrated at a temperature of 310 K. The simulations were conducted in the isothermal-isobaric (NPT) ensemble with periodic boundary conditions. Electrostatic interactions were computed using the particle mesh Ewald method (Cheatham et al., 1995). The van der Waals interactions were calculated at a cutoff and switching distances of 12 Å and 10 Å, respectively. The temperature and pressure were maintained constant using a Langevin thermostat and a Langevin barostat, respectively. All simulations were conducted for at least 20

ns using 2 fs time steps (Feller et al., 1995).

The RMSD of protein Cα atoms was calculated in each simulation. Moreover, the H-bonding occupancy was analyzed using the H-bond plugin. The cutoff distance and angle of occupancy were set to 3.5 Å and 120°, respectively. The simulation of binding free energy (ΔG_{bind}) was also calculated by MM/PBSA (Molecular Mechanics/Poisson-Boltzmann Surface Area) in the CaFE plugin. Each simulation extracted at least 5000 snapshots from the last 5 ns of the trajectories. The calculation of MM/PBSA was performed according to a methodology described previously (Hou et al., 2011).

Recombinant yeast assay

All the chemicals were purchased from Sigma-Aldrich (St. Louis, MO, USA) and dissolved in dimethyl sulfoxide (DMSO), the concentration of which did not exceed 1% (v/v) of the test chemicals. *Saccharomyces cerevisiae* recombinant yeast was purchased from Xenometrix AG (XenoScreen YES; Allschwil, Switzerland) and was genetically integrated to express hESR1 (YES). The expression plasmid of the reporter gene *lac*-Z was also inserted into the yeast, which induces the β-galactosidase enzyme. Therefore, when an agonist bound to the hESR1 in the yeast, yeast was activated and expressed β-galactosidase, which converts chlorophenol red-β-D-galactopyranoside (CPRG) into chlorophenol red (Xenometrix, 2018). Based on this principle, the yeast could be used to evaluate the estrogenic activity of chemicals; for this, we used E2 as a reference chemical. The test yeast was exposed to half-logarithmic (3.16-fold) dilutions of E2 and other chemicals. The exposure ranges were 10^{-11} to 10^{-8} M for E2, 10^{-7} to 10^{-4} M for BPA and TMBPA, and 10^{-8} to 10^{-5} M for BPFL and 4-phenylphenol, respectively. The medium containing yeast and CPRG (200 μL) was exposed to the test chemicals (2 μL) in 96-well plates and incubated at 31 °C with shaking (100 rpm) for 48 h. E2 treatment resulted in the cleavage of CPRG

into chlorophenol red by the induction of β-galactosidase. We analyzed optical density at 690 nm (OD_{690}) and 570 nm (OD_{570}) using a spectrophotometer (Tecan, Männedorf, Switzerland). Data analysis was conducted according to the yeast assay manufacturer's protocol (Xenometrix, 2018).

Cell culture, transfection, and luciferase reporter assay

The human embryonic kidney 293 cell line (HEK293, CRL-1573; ATCC, Wesel, Germany) was utilized as a transfection host for the zEsr1 construct. The HEK293 cells were cultured in Dulbecco's modified Eagle's medium without phenol red (DMEM; Thermo Scientific, Karlsruhe, Germany), with 10% fetal bovine serum (Thermo Scientific) and 1% penicillin-streptomycin (Thermo Scientific), at 37 °C and 5% CO_2.

The HEK293 cells were transduced with the pGreenFire Lenti-reporter plasmid (pGF2-ERE-rFLuc-T2A-GFP-mPGK-Puro, TR455VA-P; System Biosciences, Palo Alto, CA, USA) that encodes GFP reporter and red-shifted luciferase, under the control of ERE response elements with the puromycin resistance, according to a previously described methodology (Elegheert et al., 2018). Briefly, the cells were plated with 3×10^5 cells per well in a 6-well plate (Thermo Scientific) before transduction. After overnight culture, the old medium was aspirated and the virus-containing medium was treated with 5 μg/mL of polybrene for 8 h. Subsequently, the virus-containing medium was removed and the transduced cells were allowed to recover overnight before the addition of puromycin (10 μg/mL) for selection in the medium. In the second step, the transduced cells (HEK293-ERE) were transfected with the piggyBac transposon gene expression system. The zEsr1 expression vector was custom-cloned by vectorbuilder (pPB-Neo-CAG>zEsr1, VB210426-1022cns; Vectorbuilder Inc. Chicago, USA) and the pRP-mCherry-CAG>hyPBase plasmid (VB160216-10057; Vectorbuilder Inc) encodes the

hyperactive version of piggyBac transposase. The cells were plated with 1 x 10^5 cells per well in a 6-well plate. After overnight culture, 1 μg of the vector and 0.75 μL of the lipofectamine 3000 reagent were mixed in 250 μL of Opti-MEM medium and incubated for 15 min for DNA-lipid complex formation. The complex was treated to the wells and incubated for 6 h. Afterward, the medium was removed and the cells were allowed to recover overnight before the addition of puromycin and neomycin (10 μg/mL and 2 μg/mL, respectively). Finally, the transfected cells (HEK293-ERE-zEsr1) were collected.

The HEK293-ERE-zEsr1 cells were used to assess the estrogenic activity of chemicals. E2 was used as a reference chemical and the cells were exposed to half-logarithmic (3.16-fold) dilutions of E2 and other chemicals. The exposure ranges were 10^{-12}–10^{-9} M for E2 and 10^{-10}–10^{-5} M for other chemicals, respectively. The test chemicals were obtained with high purity (≥ 98%) from Sigma–Aldrich and were dissolved in dimethyl sulfoxide (DMSO), with a concentration not exceeding 0.5% (v/v). The cells were seeded at a rate of 1.0×10^4 cells per well on a 96-well plate. After overnight culture, the chemical solutions were treated with a ratio of 1:1 in each well containing the medium, and cultured for 24 h. The cells were lysed with passive lysis buffer (Promega, Mannheim, Germany), and the lysates were applied to evaluate Firefly luciferase activity using the Luciferase Reporter Assay System (Promega). Luminescence was measured as relative luminescence units with an integration time of 10 sec and a settling time of 1 sec using a microplate reader.

Statistical analysis

All data of the *in vitro* studies are presented as the mean of triplicate of three wells per concentration and are presented as the mean ± standard deviation. Graphs are prepared using SigmaPlot (Version 12.0, Systat Software Inc., San Jose, CA,

USA). The correlation analysis was performed using Pearson correlation test in R version 3.5.1 through RStudio Version 1.2.5042.

Results and discussion

Sequence alignment, template selection, and homology modeling

Sequence alignments of hESRs and zEsrs were obtained and are compared in Figure 1. The sequence identity between hESR1 and zEsr1 is 47% (Figure 1A). Notably, the sequence identity of LBD between hESR1 and zEsr1 increase to 62%, which indicates better conservation compared to other domains. The sequence similarity of the LBD regions between both sequences is 78%. The PCA results indicated clear separations between estrogen receptor 1 and estrogen receptor 2, regardless of the species (Figure 1B). The hESR1 and zEsr1 isoforms are closer to each other than the hESR2 and zEsr2 isoforms. The phylogenetic tree reveals the close inter-relationship of 1 and 2 isoforms of hESR and zEsr in terms of evolutionary distance metric. (Figure 1C).

Sequence alignment is a pivotal step in generating a homology model, as sequence misalignment can result in homology model errors and the generation of different models (Venclovas, 2003; Chang and Swaan, 2006). Phylogenetic analysis confirmed that zEsr1 is derived from the estrogen receptor 1 ancestral subtype and that zEsr2 isoforms belong to the estrogen receptor 2 subgroup. Moreover, the LBD is highly conserved following the DNA binding domain (Menuet et al., 2002). Consequently, the LBD sequences of hESR1 and zEsr1 were considered well conserved within the same subtype.

A homology model of zEsr1-LBD was generated using MODELLER based on sequence alignment (Figure 2). hESR1-LBD (PDB ID: 2YJA; Figure 2A) was selected as a template, with a query coverage, sequence identity, e-value, and bit score of 44%, 62.1%, 6e-109, and 327, respectively. Ten homology models were generated,

and the optimal zEsr1-LBD model was selected according to the lowest discrete optimized protein energy (DOPE score: −32,888; Figure 2B). The x-ray crystal structure of hESR1-LBD and the homology model of zEsr1-LBD are superimposed in Figure 2C. The backbone positional RMSD between the two structures was 0.162 Å, indicating that the zEsr1-LBD model has high similarity and structural comparability with the hESR1-LBD structure (Martí-Renom et al., 2000; Shehadi et al., 2020). The ligand-binding cavities when both receptors were bound to E2 are superimposed in Figure 2D. Three residues at corresponding positions of the ligand-binding cavities of hESR1 and zEsr1 were involved in hydrogen bonding and each residue of the two receptors formed hydrogen bonding interactions with the identical atoms of E2. Moreover, the distances of each corresponding hydrogen bond are comparable between the two species. Taken together, these results confirmed the reliability of the generated zEsr1-LBD and binding similarity between the hESR1- and zEsr1-LBDs.

Model validation

The generated model, including the conformation-dependent backbone geometry, was validated using PROCHECK, ERRAT, ProSA, and Verify-3D (Supplementary Table 1 and Supplementary Figure 1). PROCHECK was used to obtain a Ramachandran plot (Morris et al., 1992) for evaluating the stereochemical properties of hESR1-LBD and zEsr1-LBD, which presents the phi (φ) and psi (ψ) distributions of backbone conformation angles for each residue in a protein structure consistent with a right-handed α-helix (Supplementary Figure 1A). A good-quality model is expected to occupy over 90% of the most favorable region in the Ramachandran plot (Morris et al., 1992; Otero et al., 2010). For the plots of hESR1-LBD and zEsr1-LBD, amino acids occupied 96.6% and 97.5% of the most favorable region, respectively. None of the residues were present in the disallowed region in the plot generated for zEsr1-LBD, while 0.4% of the residues were present in the

disallowed region of the plot for hESR1-LBD, indicating that both structures were good stereochemical models. ERRAT was used to assess the relative distributions of different atom types in the test structure and determine the overall quality factor for non-covalent bonded atomic interactions, scoring exceeding 90% which resulted in 97.0% and 90.8% for hESR1-LBD and zEsr1-LBD, respectively, indicating that the backbone conformation and non-covalent bonding interactions of hESR1-LBD and zEsr1-LBD were acceptable for high-quality structure models (Supplementary Figure 1B) (Colovos and Yeates, 1993; Shamsara, 2019).

The structures were also cross-validated using ProSA-web (z-score), which resulted in -6.80 and -6.76 for hESR1-LBD and zEsr1-LBD, respectively, and plotted within the range for entire proteins determined by the Nuclear Magnetic Resonance and x-ray-derived structures (Supplementary Figure 1C). The results suggest that the prediction accuracy of the 3D protein structure models is acceptable, when compared to the previous studies (Wiederstein and Sippl, 2007; Otero et al., 2010; Shehadi et al., 2020). Finally, the Verify-3D server was used to predict the hESR1-LBD and zEsr1-LBD structures as profile-3D scores, which were presented as a table computed from the atomic coordinates of the structure (Supplementary Figure 1D). A 3D-1D score exceeding 0.2 for over 65% of a structure indicates high quality in a general manner, according to previous studies (Lüthy et al., 1992; Shamsara, 2019). The verify-3D server predicted that 79.2% of the residues in hESR1-LBD had an average 3D-1D score of > 0.2, while 78.0% of the residues in zEsr1-LBD had an average 3D-1D score of > 0.2. Both structures are quite matched their amino sequences, with high scores. Overall, the modeled zEsr1-LBD was comparatively robust and could be applied for the subsequent evaluation of binding activities.

Molecular docking and MD simulations

The docking of chemicals on hESR1-LBD and zEsr1-LBD was successfully simulated and revealed multiple docking poses for each ligand binding site. The binding poses of the docked complexes are illustrated in Figure 3. Especially, the docked complexes of E2/hESR1-LBD and E2/zEsr1-LBD exhibited an identical pattern of interactions between ligand and receptor, consisting of three hydrogen bonds and nine hydrophobic interactions. The hydrogen bonds were Glu353, Arg394, and His524 for hESR1-LBD, and Glu321, Arg362, and His492 for zEsr1-LBD. However, the interactions with BPA differed between hESR1-LBD and zEsr1-LBD. The interactions of BPA with hESR1-LBD consisted of two hydrogen bonds and nine hydrophobic interactions, while three hydrogen bonds and ten hydrophobic interactions were observed in the BPA/zEsr1-LBD complex. Notably, two hydrogen bonds (Glu353 and His524 for hESR1-LBD, and Glu321 and His492 for zEsr1-LBD) were shared between both structures. The docked complex between BPFL and hESR1-LBD consisted of one hydrogen bond and five hydrophobic interactions. Ser512 hESR1-LBD a hydrogen bond with BPFL as a hydrogen bond. The docked complex with BPFL/zEsr1-LBD exhibited one hydrogen bond, two electrostatic interactions, and five hydrophobic interactions. TMBPA exhibited the same hydrogen bonds as BPA in hESR1-LBD. Two phenolic hydroxyl groups formed hydrogen bonds with polar residues of Glu353 and His524, respectively. TMBPA formed electrostatic interaction with the Met343 residue. Only one hydrogen bond (His492) was observed in the TMBPA/zEsr1-LBD complex. Additionally, 4-phenylphenol formed the same hydrogen bonds and hydrophobic interactions in both receptors. The van der Waals interactions of only three residues differed, and the hydrogen bonds were Glu353 and Arg394 for hESR1-LBD, and Glu321 and Arg362 for zEsr1-LBD.

Before analyzing the MD simulation results, each ligand-receptor complex was evaluated for dynamic stability based on the RMSD values of all atoms

(Supplementary Figure 2 and Supplementary Figure 3). The RMSD values were between 0.8 and 2.2 Å in ligand/hESR1-LBD complexes, and between 1.6 and 4.5 Å in ligand/zEsr1-LBD complexes. All complexes favored to converge from 5 ns and reached a steady state after 10 ns equilibration. The hydrogen bond (H-bonding) occupancies between 10 and 15 ns in the MD trajectory analysis were analyzed with Glu353, Arg394, and His524 for hESR1-LBD and Glu321, Arg362, and His492 for zEsr1-LBD, respectively (Figure 4). These residues are interacted with E2 as major hydrogen bonds, as previously described (Asnake et al., 2019; Kalaiarasi et al., 2019). In contrast of TMBPA, E2, BPA, BPFL and 4-phenylphenol exhibited similar patterns in the docked complexes with hESR1-LBD and zEsr1-LBD. Considering the sum of three H-bonding occupancies, E2/hESR1- and E2/zEsr1-LBDs ratio exhibited superiority when compared with those of other chemicals, in the order of E2 > BPA > 4-phenylphenol > TMBPA > BPFL. Similar to E2, BPA formed mainly hydrogen bonds with Glu353 and His524 in hESR1-LBD, and with Glu321 and His492 in zEsr1-LBD. None of the H-bonding occupancies with the residues was observed for BPFL. High occupancy with Glu353 was observed in the TMBPA/hESR1-LBD complex, whereas high occupancy with His492 was observed in the TMBPA/zEsr1-LBD complex. Lastly, 4-phenylphenol exhibited similar H-bonding occupancy trends in both structures. Glu353 and Arg394 were observed in the hESR1-LBD complex, and Glu321 and Arg362 were observed in the zEsr1-LBD complex.

Previous studies have attempted to determine the major amino acid residues involved in ligand recognition by hESR (Pakdel and Katzenellenbogen, 1992; Danielian et al., 1993; Ekena et al., 1996). The 515-535 residue region has been identified as responsible for ligand recognition through an alanine-scanning mutagenesis assay (Pakdel and Katzenellenbogen, 1992). Consequently, Gly521, His524, Leu525, and Met528 in helix 11 were identified as the key residues for ligand

recognition (Ekena et al., 1996). The His524 residue has recently been recognized as a key player with a critical role in maintaining agonist conformation in hESR1-LBD (Cao et al., 2017; Zhang et al., 2018). Furthermore, the hydrogen bonds with Glu353 and Arg394 residues also have been reported to stabilize ligands embedded in the hESR1 cavity, thereby providing a stable recognition site (Mu et al., 2011; Miller, 2015; Lee and Barron, 2017). In the present study, hydrogen bonds with the Glu353, Arg394, and His524 residues were observed in the E2/hESR1-LBD complex, and the interactions corresponded with previously reported docking results (Cao et al., 2017; Kalaiarasi et al., 2019; Wang et al., 2020; Park et al., 2021). Collectively, the docking results of this work indicated that BPA and its analogs were located in hESR1-LBD forming diverse interactions. BPA, TMBPA, and 4-phenylphenol shared some similarity to E2 in hydrogen bonding interactions. BPA and TMBPA formed hydrogen bonds with Glu353 and His524, which were associated with the ligand recognition site. Although 4-polyphenol interacted with two other hydrogen bonds, Gly521, His524, Leu525, and Met528 in H11 formed van der Waals interactions. Two to four hydrogen bonds were observed in the BPA/hESR1-LBD complex: Glu353, Arg394, Gly521, and His524. Glu353 and His524 interactions have been commonly observed in previous studies (Delfosse et al., 2012; Li et al., 2015; Cao et al., 2017; Jeong et al., 2019; Cavaliere et al., 2020). Such differences regarding hydrogen bonds appear to be due to the different calculations and simulation methods used in different docking programs. Cao et al. (2017) docked TMBPA on hESR1-LBD and reported that TMBPA interacted as hydrogen bonds with Glu353 and His524 during MD simulations, which are consistent with our results. Several docking simulations have been conducted using zEsr1-LBD, and they have shown that E2 forms three hydrogen bonds corresponding to those (Glu321, Arg362, and His492) observed in the present study (Costache et al., 2005; Asnake et al., 2019). Mu et al. (2018) reported that BPA

forms the same hydrogen bonds as E2, which are similar to those (Glu321 and His492) observed in our results. When considering the key residues for ligand recognition in hESR1-LBD, BPA, TMBPA, and 4-phenylphenol were fitted to zEsr1-LBD and interacted with the residues for ligand recognition. Considering the similarity of their ligand recognition patterns to E2, these interactions were assumed to contribute to agonism. Similar to in hESR1-LBD, the interactions of TMBPA and 4-phenylphenol with zEsr1-LBD indicated that BPA and its analogs exhibited similar binding modes, which may explain how they mimic endogenous hormones that disrupt zebrafish endocrine system.

Binding energy analysis

To assess the binding affinity of ligand-receptor complexes, binding energies were calculated with molecular docking and the MD simulations. The binding energies of each chemical are listed in Table 1 and Supplementary Table 2. Docking simulations were conducted using CHARMm-based (CDOCKER) and AutoDock Vina, and all chemicals were docked in hESR1-LBD and zEsr1-LBD. In the hESR1-LBD simulations, the E2/hESR1-LBD complex exhibited the lowest binding energy among the test chemicals in both docking programs, while the BPFL/hESR1-LBD complex exhibited the highest energy. The binding energies in hESR1-LBD were ranked as follows: E2 > TMBPA ≥ BPA > 4-phenylphenol > BPFL. In the zEsr1-LBD simulations, a similar pattern to hESR1-LBD was observed, with the lowest binding energy occurring for the E2/zEsr1-LBD complex, and the highest occurring for the BPFL/hESR1-LBD complex among the test chemicals. The binding energies were ranked as follows: E2 > BPA ≒ TMBPA > 4-phenylphenol > BPFL. The steady state of 10 and 15 ns MD simulations revealed the following order, TMBPA > E2 > BPA > 4-phenylphenol > BPFL, in which TMBPA revealed a lower binding free energy than E2 in the hESR1. For the zEsr1 complexes, the binding free energies were ranked as

follows: E2 > BPA > TMBPA > 4-phenylphenol > BPFL. The binding energies differed according to the chemicals used. The docking programs exhibited similar binding energy patterns, and they corresponded with the results of previous studies (Makarova et al., 2016; Jeong et al., 2019; Cavaliere et al., 2020). BPA and its analogs were docked, and their binding energies with hESR1-LBD were compared. E2/hESR1-LBD exhibited lower binding energy than BPA and its substitutes. Cavaliere et al. (2020) reported the same binding energy pattern for hESR1-LBD (E2 > TMBPA > BPA). Makarova et al. (2016) simulated E2 and BPA docking on simulated hESR1-LBD and zEsr1-LBD using AutoDock, and E2 exhibited lower binding energy than BPA. The binding energies were -11.5 and -7.73 kcal/mol for hESR1-LBD and -11.0 and -7.56 kcal/mol for zEsr1-LBD, respectively. The E2/hESR1-LBD manifested lower binding free energy than BPA/hESR1-LBD using MM/PBSA and MMGBSA methods (Li et al., 2015; Li et al., 2018). Notably, the TMBPA/hESR1-LBD displayed a lower binding free energy than the E2 complex during MD simulation, which is not consistent with docking calculation. It can be explained by van der Waals and hydrophobic interactions (Supplementary Table 2). The calculated van der Waals (ΔG_{vdw}) and non-polar solvation (ΔG_{SA}) of TMBPA interactions revealed the lowest energies among the complexes. Previous reports have shown that the energies of the apolar ($\Delta G_{vdw} + \Delta G_{SA}$) and electrostatic ($\Delta G_{elec}$) components dominantly contribute to the estimate of binding free energy in MM/PBSA (Tan et al., 2006; Verma et al., 2016). Therefore, TMBPA resulted in a lower binding free energy than E2 in hESR1-LBD. Whereas, the TMBPA-zEsr1-LBD complex exhibited a higher binding free energy than E2 due to the electrostatic interactions. The electrostatic energy was markedly lower in zEsr1-LBD than in the hESR1-LBD complex. Collectively, each complex showed different binding energies and the patterns were confirmed by docking programs and MD simulation.

Comparison of in silico and in vitro experiments

The *in silico* and *in vitro* results were compared to evaluate their correlation, as shown in Figure 5. The human estrogenic activities of BPA and its analogs were evaluated by conducting an *in vitro* reporter gene assay (Figure 5A). The maximum concentration of each chemical with a non-toxic effect on the yeast strain was selected based on the results of the cytotoxicity test. E2 was used as the reference chemical and exhibited a dose response depending on the concentration. BPA and its analogs also exhibited dose-response curves, excluding BPFL. The EC_{50} values for E2, BPA, TMBPA, and 4-phenylphenol were 1.25, 14,657, 10,216, and 4,594 nM, respectively. The maximal induction rates of BPA and its analogs were ranked in the following order: BPA > TMBPA > 4-phenylphenol > BPFL. Even though the EC_{50} value of BPA was higher than those of TMBPA and 4-phenylphenol, BPA exhibited the highest induction rate (90.7%) at the maximum concentration except E2. Similar results have been reported in other reporter gene studies (Sun et al., 2008; Cao et al., 2017; Pelch et al., 2019; Bergmann et al., 2020). TMBPA exhibited lower EC_{20} and EC_{50} values than BPA; however, the estrogenic activity at the maximum concentration of BPA was higher than that of TMBPA (Cao et al., 2017; Pelch et al., 2019). Two studies reported that the EC_{50} value of 4-phenylphenol is lower than that of BPA (Sun et al., 2008; Bergmann et al., 2020). Conversely, Li et al. (2010) reported a higher EC_{50} value for 4-phenylphenol than for BPA. Such differences can be attributed to the different reporter systems, and the different host cells and their cytotoxicity and ligand-binding affinity. Our *in vitro* assay showed that BPFL and 4-phenylphenol appeared to be more cytotoxic (> 10 μM) than BPA and TMBPA (> 100 μM). Keminer et al. (2020) recently conducted a ligand-binding assay using a commercially available fluorescence polarization-based technique. BPA inhibited the fluorescent ligand by 61.2%, followed by 4-phenylphenol (53.1%), TMBPA (24.2%), and BPFL

(-2.06%). Therefore, it seems that BPA exhibited the highest estrogenic activity compared to BPA analogs, despite the lower EC_{50} values of TMBPA and 4-phenylphenol.

In the present study, zebrafish estrogenic activities of BPA and its analogs were evaluated using an *in vitro* reporter gene assay (Figure 5B). The maximum concentrations of compounds with a non-toxic effect on the cells were selected based on the results of the cytotoxicity test. E2, BPA, and 4-phenylphenol exhibited dose-response curves. The EC_{50} values for E2, BPA, and 4-phenylphenol were 0.09, 583, and 9,787 nM, respectively. TMBPA induced weak estrogenic activity (16.6% as the maximal induction), which was different from the estrogenic activity in the human *in vitro* assay. The maximal induction rates of BPA and its analogs were ranked in the following order: BPA > 4-phenylphenol > TMBPA > BPFL. Each chemical exhibited different estrogenic activities in this reporter assay. None of the previous studies showed estrogenic activity with BPFL, TMBPA, and 4-phenylphenol in zEsr1, while estrogenic activity has been observed with BPA (Cosnefroy et al., 2012; Le Fol et al., 2017; Pinto et al., 2019).

Lastly, the *in silico* and *in vitro* results were compared to evaluate their correlation. All the factors computed by *in silico* experiments revealed moderate or high correlations with *in vitro* results (Figure 5C and 5D). High correlation was observed between Cdocker and AutoDock Vina (r^2 = 0.84 for hESR1 and r^2 = 0.77 for zEsr1). Notably, the H-bonding occupancy exhibited high correlations with *in vitro* results (r^2 = 0.81 for hESR1 and r^2 = 0.87 for zEsr1). The result indicates that hydrogen bond interactions with certain residues have pivotal roles for ligand recognition and its activation. The interaction of modelled zEsr1 with TMBPA resulted in relatively poor correlations compared to *in vitro* results than those of hESR1 although the TMBPA complex in both receptors revealed comparable binding

free energies compared with BPA and 4-phenylphenol interactions. The *in vitro* results of weak estrogenic activity of TMBPA can be explained by the MM/PBSA calculated lowest energies in van der Waals and non-polar solvation among the complexes. In addition, TMBPA formed a hydrogen bond with the His492 residue in the docking programs and the MD simulation. The residue is considered to be critical in ligand recognition and maintenance of the agonist conformation (Babu et al., 2012; Shehadi et al., 2020). The results are inconsistent with previous reports and the present *in vitro* result. However, the inconsistency can be elucidated with other residues such as Glu353 and Arg394 in hESR1-LBD. Considering the reported functions of Glu353 and Arg394 residues, and the results in H-bonding occupancy, we speculate that even though the His492 residue plays critical roles, other residues such as Glu321 and Arg362 are necessary as well for the complex stabilization and its activation. For these reasons, it seems TMBPA induced different estrogenic activities on human ESRα and zebrafish ESRα. Overall, the present study found a good agreement between the results from *in silico* and *in vitro* approaches using the hESR1-LBD and zEsr1-LBD structures. The structures can be useful for screening EDCs that have potential estrogenic disruptive activities. However, the current approach also reveals some limitations, which are needed to consider for better prediction. A relatively smaller scale of the test and limited sampling conditions in pose prediction and approximated scoring, might cause poor correlation of results with experimental *in vitro* data. Moreover, this structure only predicts estrogenic activity between the LBD and a ligand, thereby it is impossible to predict estrogenic activities related to other mechanisms or domains. In light of these limitations, more studies with diverse ligands are necessary to draw a solid conclusion, and detailed analyses of binding energy and interaction modes are required to predict estrogenic activity. Our future

study will be the assessment of other EDCs and the investigation to reveal other mechanisms inducing (anti)estrogenic activities.

Conclusion

As the 3D structure of zebrafish ESRα is not available, a homology-based 3D model of zEsr1-LBD was constructed and validated using PROCHECK, ERRAT, ProSA, and Verify-3D tools, which have suitable models to represent the 3D structure. After validation, BPA and its analogs were docked on zEsr1- and hESR1-LBDs. MD simulation was conducted to understand the dynamic behavior of each complex and provided noteworthy complementary with molecular docking. Several BPA and its analogs were bound to both models with an orientation as E2 in both structures. Additionally, the *in vitro* results demonstrated that the *in silico* and *in vitro* results were in good agreement with moderate to high correlations. Therefore, the combined *in silico* and *in vitro* approaches provide useful prediction models for identifying EDCs by taking into account the difference between the two species.

Supporting Information—The Supporting information are available on the Wiley Online Library at DOI: 10.1002/etc.xxxx.

Acknowledgment—This research was supported by the National Research Council of Science & Technology (NST) grant by the Korea government (MSIP) (No. CAP-17-01-KIST Europe) and the Korea Institute of Science and Technology Europe Basic Research Program (Project no. 12201).

Disclaimer—The authors declare that they have no known competing financial interests or personal relationships that could have appeared to influence the work reported in this paper

Data availability— The authors confirm that the data supporting the findings of this study are available within the article and its Supplementary Information. All data of this study are available from

https://drive.google.com/drive/folders/1B3LnXhZQDRkgXs6YykEcduuO0j9IMWQw?usp=sharing.

Author contributions statement—Chang Gyun Park – writing - original draft, data curation, formal analysis, writing - review & editing. Nancy Singh – data curation, formal analysis, resources, methodology, writing - review & editing. Chang Seon Ryu – writing - original draft, data curation, formal analysis, writing - review & editing. Ju Yong Yoon – formal analysis, methodology, writing - review & editing. Maranda Esterhuizen – conceptualization, investigation, methodology, writing - review & editing. Young Jun Kim – writing - original draft, conceptualization, funding acquisition, investigation, methodology, writing - review & editing. All persons who meet authorship criteria are listed as authors, and all authors certify that they have participated sufficiently in the work to take public responsibility for the content, including participation in the concept, design, analysis, writing, or revision of the manuscript. Furthermore, each author certifies that this material or similar material has not been and will not be submitted to or published in any other publication before its appearance in Environmental Toxicology and Chemistry. All authors contributed equally to this study. The final version of the manuscript has been approved by all authors.

References

Altschul, S.F., Gish, W., Miller, W., Myers, E.W., Lipman, D.J. (1990). Basic local alignment search tool. *Journal of Molecular Biology*, *215*(3), 403-410.

Asnake, S., Modig, C., Olsson, P.-E. (2019). Species differences in ligand interaction and activation of estrogen receptors in fish and human. *The Journal of Steroid Biochemistry and Molecular Biology*, *195*, 105450.

Babu, S., Vellore, N.A., Kasibotla, A.V., Dwayne, H.J., Stubblefield, M.A., Uppu, R.M. (2012). Molecular docking of bisphenol A and its nitrated and chlorinated

metabolites onto human estrogen-related receptor-gamma. *Biochemical and Biophysical Research Communications*, *426*(2), 215-220.

Banaderakhshan, R., Kemp, P., Breul, L., Steinbichl, P., Hartmann, C., Fürhacker, M. (2022). Bisphenol A and its alternatives in Austrian thermal paper receipts, and the migration from reusable plastic drinking bottles into water and artificial saliva using UHPLC-MS/MS. *Chemosphere*, *286*, 131842.

Bardet, P.L., Horard, B., Robinson-Rechavi, M., Laudet, V., Vanacker, J.M. (2002). Characterization of oestrogen receptors in zebrafish (*Danio rerio*). *Journal of Molecular Endocrinology*, *28*(3), 153-163.

Barkhem, T., Nilsson, S., Gustafsson, J.A. (2004). Molecular mechanisms, physiological consequences and pharmacological implications of estrogen receptor action. *American Journal of Pharmacogenomics*, *4*(1), 19-28.

Barros, R.P., Gustafsson, J. (2011). Estrogen receptors and the metabolic network. *Cell Metabolism*, *14*(3), 289-299.

Bergmann, A.J., Simon, E., Schifferli, A., Schönborn, A., Vermeirssen, E.L.M. (2020). Estrogenic activity of food contact materials—evaluation of 20 chemicals using a yeast estrogen screen on HPTLC or 96-well plates. *Analytical and Bioanalytical Chemistry*, *412*(19), 4527-4536.

Cao, H., Wang, F., Liang, Y., Wang, H., Zhang, A., Song, M. (2017). Experimental and computational insights on the recognition mechanism between the estrogen receptor α with bisphenol compounds. *Archives of Toxicology*, *91*(12), 3897-3912.

Cavaliere, F., Lorenzetti, S., Cozzini, P. (2020). Molecular modelling methods in food safety: Bisphenols as case study. *Food and Chemical Toxicology*, *137*, 111116.

Chafi, S., Azzouz, A., Ballesteros, E. (2022). Occurrence and distribution of endocrine disrupting chemicals and pharmaceuticals in the river Bouregreg (Rabat, Morocco). *Chemosphere*, *287*, 132202.

Chang, C., Swaan, P.W. (2006). Computational approaches to modeling drug transporters. *European Journal of Pharmaceutical Sciences*, *27*(5), 411-424.

Cheatham, T.E., III, Miller, J.L., Fox, T., Darden, T.A., Kollman, P.A. (1995). Molecular dynamics simulations on solvated biomolecular systems: the particle mesh Ewald method leads to stable trajectories of DNA, RNA, and Proteins. *Journal of the American Chemical Society*, *117*(14), 4193-4194.

Chen, D., Kannan, K., Tan, H., Zheng, Z., Feng, Y.-L., Wu, Y., Widelka, M. (2016). Bisphenol analogues other than BPA: environmental occurrence, human exposure, and toxicity—a review. *Environmental Science & Technology*, *50*(11), 5438-5453.

Colovos, C., Yeates, T.O. (1993). Verification of protein structures: patterns of nonbonded atomic interactions. *Protein Science*, *2*(9), 1511-1519.

Cosnefroy, A., Brion, F., Maillot-Maréchal, E., Porcher, J.M., Pakdel, F., Balaguer, P., Aït-Aïssa, S. (2012). Selective activation of zebrafish estrogen receptor subtypes by chemicals by using stable reporter gene assay developed in a zebrafish liver cell line. *Toxicological Sciences*, *125*(2), 439-449.

Costache, A.D., Pullela, P.K., Kasha, P., Tomasiewicz, H., Sem, D.S. (2005). Homology-modeled ligand-binding domains of zebrafish estrogen receptors alpha, beta1, and beta2: from in silico to in vivo studies of estrogen interactions in *Danio rerio* as a model system. *Molecular Endocrinology*, *19*(12), 2979-2990.

Dahlman-Wright, K., Cavailles, V., Fuqua, S.A., Jordan, V.C., Katzenellenbogen, J.A., Korach, K.S., Maggi, A., Muramatsu, M., Parker, M.G., Gustafsson, J.A. (2006). International union of pharmacology. LXIV. estrogen receptors. *Pharmacological Reviews*, *58*(4), 773-781.

Danielian, P.S., White, R., Hoare, S.A., Fawell, S.E., Parker, M.G. (1993). Identification of residues in the estrogen receptor that confer differential sensitivity to estrogen and hydroxytamoxifen. *Molecular Endocrinology*, *7*(2), 232-240.

Delfosse, V., Grimaldi, M., Pons, J.L., Boulahtouf, A., le Maire, A., Cavailles, V., Labesse, G., Bourguet, W., Balaguer, P. (2012). Structural and mechanistic insights into bisphenols action provide guidelines for risk assessment and discovery of bisphenol A substitutes. *Proceedings of the National Academy of Sciences of the United States of America*, *109*(37), 14930-14935.

Ekena, K., Weis, K.E., Katzenellenbogen, J.A., Katzenellenbogen, B.S. (1996). Identification of amino acids in the hormone binding domain of the human estrogen receptor important in estrogen binding. *Journal of Biological Chemistry*, *271*(33), 20053-20059.

Elegheert, J., Behiels, E., Bishop, B., Scott, S., Woolley, R.E., Griffiths, S.C., Byrne, E.F.X., Chang, V.T., Stuart, D.I., Jones, E.Y., Siebold, C., Aricescu, A.R. (2018). Lentiviral transduction of mammalian cells for fast, scalable and high-level production of soluble and membrane proteins. *Nature Protocols*, *13*(12), 2991-3017.

Feller, S.E., Zhang, Y., Pastor, R.W., Brooks, B.R. (1995). Constant pressure molecular dynamics simulation: The Langevin piston method. *The Journal of Chemical Physics*, *103*(11), 4613-4621.

Geens, T., Aerts, D., Berthot, C., Bourguignon, J.P., Goeyens, L., Lecomte, P., Maghuin-Rogister, G., Pironnet, A.M., Pussemier, L., Scippo, M.L., Van Loco, J., Covaci, A. (2012). A review of dietary and non-dietary exposure to bisphenol-A. *Food and Chemical Toxicology*, *50*(10), 3725-3740.

Hawkins, M.B., Thornton, J.W., Crews, D., Skipper, J.K., Dotte, A., Thomas, P. (2000). Identification of a third distinct estrogen receptor and reclassification of estrogen receptors in teleosts. *Proceedings of the National Academy of Sciences of the United States of America*, *97*(20), 10751.

Heldring, N., Pike, A., Andersson, S., Matthews, J., Cheng, G., Hartman, J., Tujague, M., Ström, A., Treuter, E., Warner, M., Gustafsson, J.A. (2007). Estrogen receptors:

how do they signal and what are their targets. *Physiological Reviews*, *87*(3), 905-931.

Hewitt, S.C., Winuthayanon, W., Korach, K.S. (2016). What's new in estrogen receptor action in the female reproductive tract. *Journal of Molecular Endocrinology*, *56*(2), R55-71.

Hou, T., Wang, J., Li, Y., Wang, W. (2011). Assessing the performance of the MM/PBSA and MM/GBSA methods. 1. The accuracy of binding free energy calculations based on molecular dynamics simulations. *Journal of Chemical Information and Modeling*, *51*(1), 69-82.

Humphrey, W., Dalke, A., Schulten, K. (1996). VMD: visual molecular dynamics. *Journal of Molecular Graphics*, *14*(1), 33-38.

Jeong, J., Kim, H., Choi, J. (2019). In silico molecular docking and In vivo validation with *Caenorhabditis elegans* to discover molecular initiating events in adverse outcome pathway framework: case study on endocrine-disrupting chemicals with estrogen and androgen receptors. *International Journal of Molecular Sciences*, *20*(5), 1209.

Jin, H., Zhu, L. (2016). Occurrence and partitioning of bisphenol analogues in water and sediment from Liaohe River Basin and Taihu Lake, China. *Water Research*, *103*, 343-351.

Jin, M., Dang, J., Paudel, Y.N., Wang, X., Wang, B., Wang, L., Li, P., Sun, C., Liu, K. (2021). The possible hormetic effects of fluorene-9-bisphenol on regulating hypothalamic-pituitary-thyroid axis in zebrafish. *Science of The Total Environment*, *776*, 145963.

Jorgensen, W.L., Chandrasekhar, J., Madura, J.D., Impey, R.W., Klein, M.L. (1983). Comparison of simple potential functions for simulating liquid water. *The Journal of Chemical Physics*, *79*(2), 926-935.

Kalé, L., Skeel, R., Bhandarkar, M., Brunner, R., Gursoy, A., Krawetz, N., Phillips, J.,

Shinozaki, A., Varadarajan, K., Schulten, K. (1999). NAMD2: greater scalability for parallel molecular dynamics. *Journal of Computational Physics*, *151*(1), 283-312.

Kalaiarasi, C., Manjula, S., Kumaradhas, P. (2019). Combined quantum mechanics/molecular mechanics (QM/MM) methods to understand the charge density distribution of estrogens in the active site of estrogen receptors. *RSC Advances*, *9*(69), 40758-40771.

Kang, J.H., Asai, D., Katayama, Y. (2007). Bisphenol A in the aquatic environment and its endocrine-disruptive effects on aquatic organisms. *Critical Reviews in Toxicology*, *37*(7), 607-625.

Kari, G., Rodeck, U., Dicker, A.P. (2007). Zebrafish: an emerging model system for human disease and drug discovery. *Clinical Pharmacology & Therapeutics*, *82*(1), 70-80.

Keminer, O., Teigeler, M., Kohler, M., Wenzel, A., Arning, J., Kaßner, F., Windshügel, B., Eilebrecht, E. (2020). A tiered high-throughput screening approach for evaluation of estrogen and androgen receptor modulation by environmentally relevant bisphenol A substitutes. *Science of The Total Environment*, *717*, 134743.

Khalid, A.B., Krum, S.A. (2016). Estrogen receptors alpha and beta in bone. *Bone*, *87*, 130-135.

Kovats, S. (2015). Estrogen receptors regulate innate immune cells and signaling pathways. *Cellular Immunology*, *294*(2), 63-69.

Kumar, R., Zakharov, M.N., Khan, S.H., Miki, R., Jang, H., Toraldo, G., Singh, R., Bhasin, S., Jasuja, R. (2011). The dynamic structure of the estrogen receptor. *Journal of Amino Acids*, *2011*, 812540.

Lüthy, R., Bowie, J.U., Eisenberg, D. (1992). Assessment of protein models with three-dimensional profiles. *Nature*, *356*(6364), 83-85.

Le Fol, V., Ait-Aissa, S., Sonavane, M., Porcher, J.-M., Balaguer, P., Cravedi, J.-P.,

Zalko, D., Brion, F. (2017). In vitro and in vivo estrogenic activity of BPA, BPF and BPS in zebrafish-specific assays. *Ecotoxicology and Environmental Safety*, *142*, 150-156.

Lee, S., Barron, M.G. (2017). Structure-based understanding of binding affinity and mode of estrogen receptor α agonists and antagonists. *PloS ONE*, *12*(1), e0169607-e0169607.

Li, L., Wang, Q., Zhang, Y., Niu, Y., Yao, X., Liu, H. (2015). The molecular mechanism of bisphenol A (BPA) as an endocrine disruptor by interacting with nuclear receptors: insights from molecular dynamics (MD) simulations. *PloS ONE*, *10*(3), e0120330-e0120330.

MacRae, C.A., Peterson, R.T. (2015). Zebrafish as tools for drug discovery. *Nature Reviews Drug Discovery*, *14*(10), 721-731.

Makarova, K., Siudem, P., Zawada, K., Kurkowiak, J. (2016). Screening of toxic effects of bisphenol A and products of Its degradation: Zebrafish (*Danio rerio*) embryo test and molecular docking. *Zebrafish*, *13*(5), 466-474.

Martí-Renom, M.A., Stuart, A.C., Fiser, A., Sánchez, R., Melo, F., Sali, A. (2000). Comparative protein structure modeling of genes and genomes. *Annual Review of Biophysics and Biomolecular Structure*, *29*, 291-325.

Mathieu-Denoncourt, J., Wallace, S.J., de Solla, S.R., Langlois, V.S. (2015). Plasticizer endocrine disruption: highlighting developmental and reproductive effects in mammals and non-mammalian aquatic species. *General and Comparative Endocrinology*, *219*, 74-88.

Menuet, A., Pellegrini, E., Anglade, I., Blaise, O., Laudet, V., Kah, O., Pakdel, F. (2002). Molecular characterization of three estrogen receptor forms in zebrafish: binding characteristics, transactivation properties, and tissue distributions. *Biology of Reproduction*, *66*(6), 1881-1892.

Mi, P., Zhang, Q.-P., Zhang, S.-H., Wang, C., Zhang, S.-Z., Fang, Y.-C., Gao, J.-Z., Feng, D.-F., Chen, D.-Y., Feng, X.-Z. (2019). The effects of fluorene-9-bisphenol on female zebrafish (*Danio rerio*) reproductive and exploratory behaviors. *Chemosphere*, *228*, 398-411.

Miller, C. (2015). *A brief on the structure and function of estrogen receptor alpha (BCMB8010 Enzyme Project)*. https://doi.org/10.13140/RG.2.1.4082.5044.

Mills, L.J., Chichester, C. (2005). Review of evidence: are endocrine-disrupting chemicals in the aquatic environment impacting fish populations? *Science of The Total Environment*, *343*(1-3), 1-34.

Montes-Grajales, D., Olivero-Verbel, J. (2013). Computer-aided identification of novel protein targets of bisphenol A. *Toxicology Letters*, *222*(3), 312-320.

Morris, A.L., MacArthur, M.W., Hutchinson, E.G., Thornton, J.M. (1992). Stereochemical quality of protein structure coordinates. *Proteins*, *12*(4), 345-364.

Mu, Y., Peng, S., Zhang, A., Wang, L. (2011). Role of pocket flexibility in the modulation of estrogen receptor alpha by key residue arginine 394. *Environmental Toxicology and Chemistry*, *30*(2), 330-336.

Otero, J.M., Papadakis, M.A., Udatha, D.B., Nielsen, J., Panagiotou, G. (2010). Yeast biological networks unfold the interplay of antioxidants, genome and phenotype, and reveal a novel regulator of the oxidative stress response. *PLoS ONE*, *5*(10), e13606.

Pakdel, F., Katzenellenbogen, B.S. (1992). Human estrogen receptor mutants with altered estrogen and antiestrogen ligand discrimination. *Journal of Biological Chemistry*, *267*(5), 3429-3437.

Park, C.G., Jung, K.C., Kim, D.-H., Kim, Y.J. (2021). Monohaloacetonitriles induce cytotoxicity and exhibit different mode of action in endocrine disruption. *Science of The Total Environment*, *761*, 143316.

Paterni, I., Granchi, C., Katzenellenbogen, J.A., Minutolo, F. (2014). Estrogen

receptors alpha (ERα) and beta (ERβ): subtype-selective ligands and clinical potential. *Steroids*, *90*, 13-29.

Pelch, K.E., Li, Y., Perera, L., Thayer, K.A., Korach, K.S. (2019). Characterization of estrogenic and androgenic activities for bisphenol A-like chemicals (BPs): in vitro estrogen and androgen receptors transcriptional activation, gene regulation, and binding profiles. *Toxicological Sciences*, *172*(1), 23-37.

Phillips, C., Roberts, L.R., Schade, M., Bazin, R., Bent, A., Davies, N.L., Moore, R., Pannifer, A.D., Pickford, A.R., Prior, S.H., Read, C.M., Scott, A., Brown, D.G., Xu, B., Irving, S.L. (2011). Design and structure of stapled peptides binding to estrogen receptors. *Journal of the American Chemical Society*, *133*(25), 9696-9699.

Phillips, J.C., Braun, R., Wang, W., Gumbart, J., Tajkhorshid, E., Villa, E., Chipot, C., Skeel, R.D., Kalé, L., Schulten, K. (2005). Scalable molecular dynamics with NAMD. *Journal of Computational Chemistry*, *26*(16), 1781-1802.

Pinto, C., Hao, R., Grimaldi, M., Thrikawala, S., Boulahtouf, A., Aït-Aïssa, S., Brion, F., Gustafsson, J., Balaguer, P., Bondesson, M. (2019). Differential activity of BPA, BPAF and BPC on zebrafish estrogen receptors in vitro and in vivo. *Toxicology and Applied Pharmacology*, *380*, 114709.

Procter, J.B., Carstairs, G.M., Soares, B., Mourão, K., Ofoegbu, T.C., Barton, D., Lui, L., Menard, A., Sherstnev, N., Roldan-Martinez, D., Duce, S., Martin, D.M.A., Barton, G.J. (2021). Alignment of biological sequences with Jalview. *Methods in Molecular Biology*, *2231*, 203-224.

Rochester, J.R. (2013). Bisphenol A and human health: a review of the literature. *Reproductive Toxicology*, *42*, 132-155.

Rosenmai, A.K., Dybdahl, M., Pedersen, M., Alice van Vugt-Lussenburg, B.M., Wedebye, E.B., Taxvig, C., Vinggaard, A.M. (2014). Are structural analogues to bisphenol A safe alternatives? *Toxicological Sciences*, *139*(1), 35-47.

Shamsara, J. (2019). Homology modeling of 5-alpha-reductase 2 using available experimental data. *Interdisciplinary Sciences, Computational Life Sciences*, *11*(3), 475-484.

Shehadi, I.A., Rashdan, H.R.M., Abdelmonsef, A.H. (2020). Homology modeling and virtual screening studies of antigen MLAA-42 protein: identification of novel drug candidates against leukemia—an in silico approach. *Computational and Mathematical Methods in Medicine*, *2020*, 8196147.

Shen, M., Shi, H. (2015). Sex hormones and their receptors regulate liver energy homeostasis. *International Journal of Endocrinology*, *2015*, 294278.

Shen, M.Y., Sali, A. (2006). Statistical potential for assessment and prediction of protein structures. *Protein Science*, *15*(11), 2507-2524.

Sliwoski, G., Kothiwale, S., Meiler, J., Lowe, E.W., Jr. (2013). Computational methods in drug discovery. *Pharmacological reviews*, *66*(1), 334-395.

Sun, H., Xu, X.-L., Qu, J.-H., Hong, X., Wang, Y.-B., Xu, L.-C., Wang, X.-R. (2008). 4-Alkylphenols and related chemicals show similar effect on the function of human and rat estrogen receptor α in reporter gene assay. *Chemosphere*, *71*(3), 582-588.

Tan, J.J., Chen, W.Z., Wang, C.X. (2006). Investigating interactions between HIV-1 gp41 and inhibitors by molecular dynamics simulation and MM–PBSA/GBSA calculations. *Journal of Molecular Structure*, *766*(2), 77-82.

Trott, O., Olson, A.J. (2010). AutoDock Vina: improving the speed and accuracy of docking with a new scoring function, efficient optimization, and multithreading. *Journal of computational chemistry*, *31*(2), 455-461.

Usman, A., Ahmad, M. (2016). From BPA to its analogues: Is it a safe journey? *Chemosphere*, *158*, 131-142.

Venclovas, C. (2003). Comparative modeling in CASP5: progress is evident, but alignment errors remain a significant hindrance. *Proteins*, *53*, 380-388.

Verma, S., Grover, S., Tyagi, C., Goyal, S., Jamal, S., Singh, A., Grover, A. (2016). Hydrophobic Interactions Are a Key to MDM2 Inhibition by Polyphenols as Revealed by Molecular Dynamics Simulations and MM/PBSA Free Energy Calculations. *PloS ONE*, *11*(2), e0149014-e0149014.

Wang, T., Wang, Y., Zhuang, X., Luan, F., Zhao, C., Cordeiro, M.N.D.S. (2020). Interaction of coumarin phytoestrogens with ERα and ERβ: a molecular dynamics simulation study. *Molecules*, *25*(5), 1165.

Webb, B., Sali, A. (2016). Comparative protein structure modeling using MODELLER. *Current Protocols in Bioinformatics*, *54*, 5.6.1-5.6.37.

Wiederstein, M., Sippl, M.J. (2007). ProSA-web: interactive web service for the recognition of errors in three-dimensional structures of proteins. *Nucleic Acids Research*, *35*, W407-410.

Wu, G., Robertson, D.H., Brooks Iii, C.L., Vieth, M. (2003). Detailed analysis of grid-based molecular docking: A case study of CDOCKER—A CHARMm-based MD docking algorithm. *Journal of Computational Chemistry*, *24*(13), 1549-1562.

Xenometrix (2018). *XenoScreen YES/YAS instructions for use*. [cited 2022 January 10]. Available from: https://www.aniara.com/mm5/PDFs/IFU/IFU_AN05-233-Y.pdf.

Zhang, J., Li, T., Wang, T., Yuan, C., Zhong, S., Guan, T., Li, Z., Wang, Y., Yu, H., Luo, Q., Wang, Y., Zhang, T. (2018). Estrogenicity of halogenated bisphenol A: in vitro and in silico investigations. *Archives of Toxicology*, *92*(3), 1215-1223.

Zhang, Y., Zhou, J.L. (2005). Removal of estrone and 17β-estradiol from water by adsorption. *Water Research*, *39*(16), 3991-4003.

Zhang, Z., Hu, Y., Guo, J., Yu, T., Sun, L., Xiao, X., Zhu, D., Nakanishi, T., Hiromori, Y., Li, J., Fan, X., Wan, Y., Cheng, S., Li, J., Guo, X., Hu, J. (2017). Fluorene-9-bisphenol is anti-oestrogenic and may cause adverse pregnancy outcomes in mice. *Nature Communications*, *8*(1), 14585.

FIGURE CAPTIONS

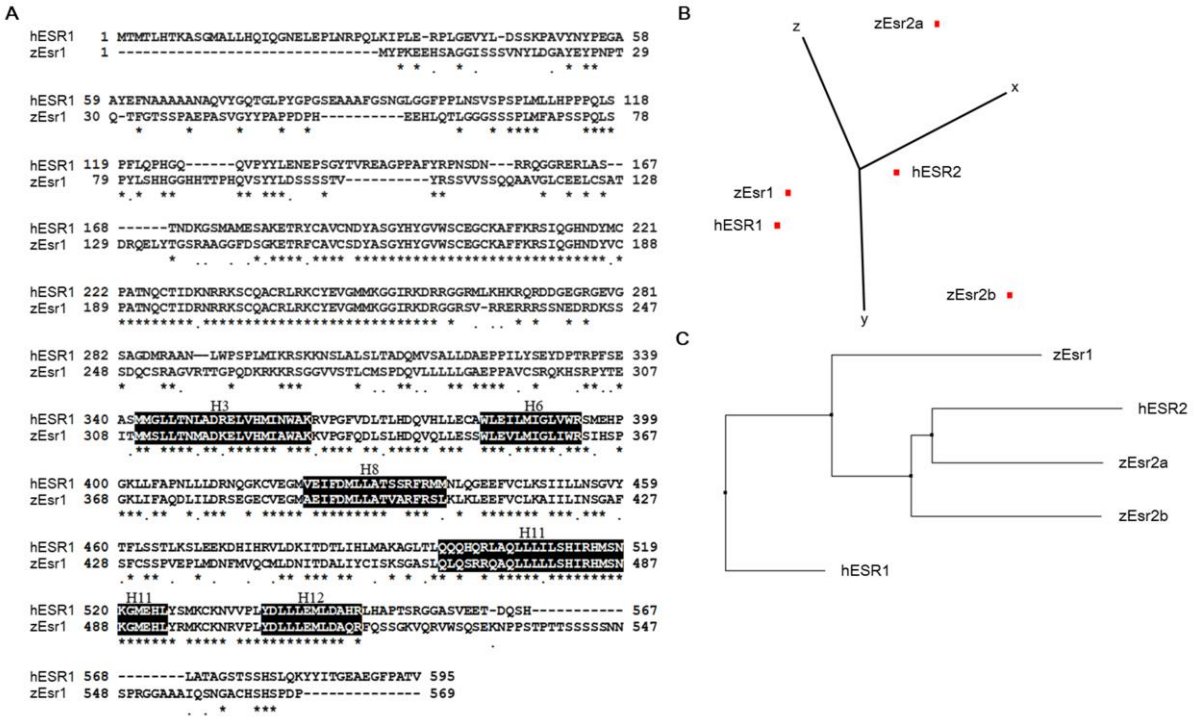

Figure 1. Sequence alignment comparison. (A) Sequence alignment between human estrogen receptor 1 (hESR1) and zebrafish estrogen receptor 1 (zEsr1). The conserved amino acids are marked with asterisks and similar properties between different amino acids are marked as dots. The helices surrounding the ligand-binding cavity are colored black in the E/F domain. Gaps are denoted with a hyphen. (B) Principal component analysis (PCA) of human and zebrafish estrogen receptors. (C) Phylogenetic analysis showing the relationships between human and zebrafish estrogen receptors.

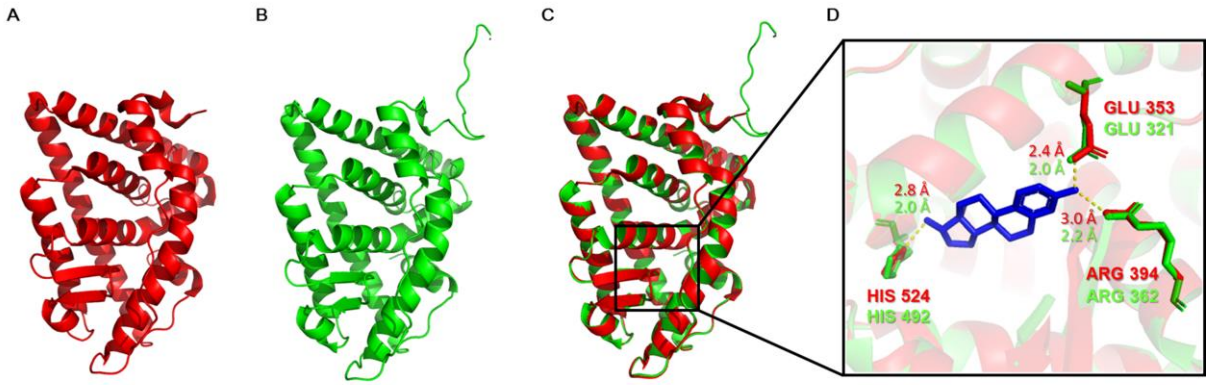

Figure 2. 3D ligand-binding domain structures of the hESR1 and modeled zEsr1. (A) Ligand-binding domain of human estrogen receptor 1 (hESR1-LBD; PDB:2YJA). (B) Ligand-binding domain of zebrafish estrogen receptor 1 (zEsr1-LBD) generated by homology modeling using MODELLER. (C) Superimposed images of hESR1-LBD (red) and zEsr1-LBD (green). (D) Hydrogen bond interactions of 17β-estradiol (E2) with both structures. Red and green residues indicate hESR1-LBD and zEsr1-LBD, respectively.

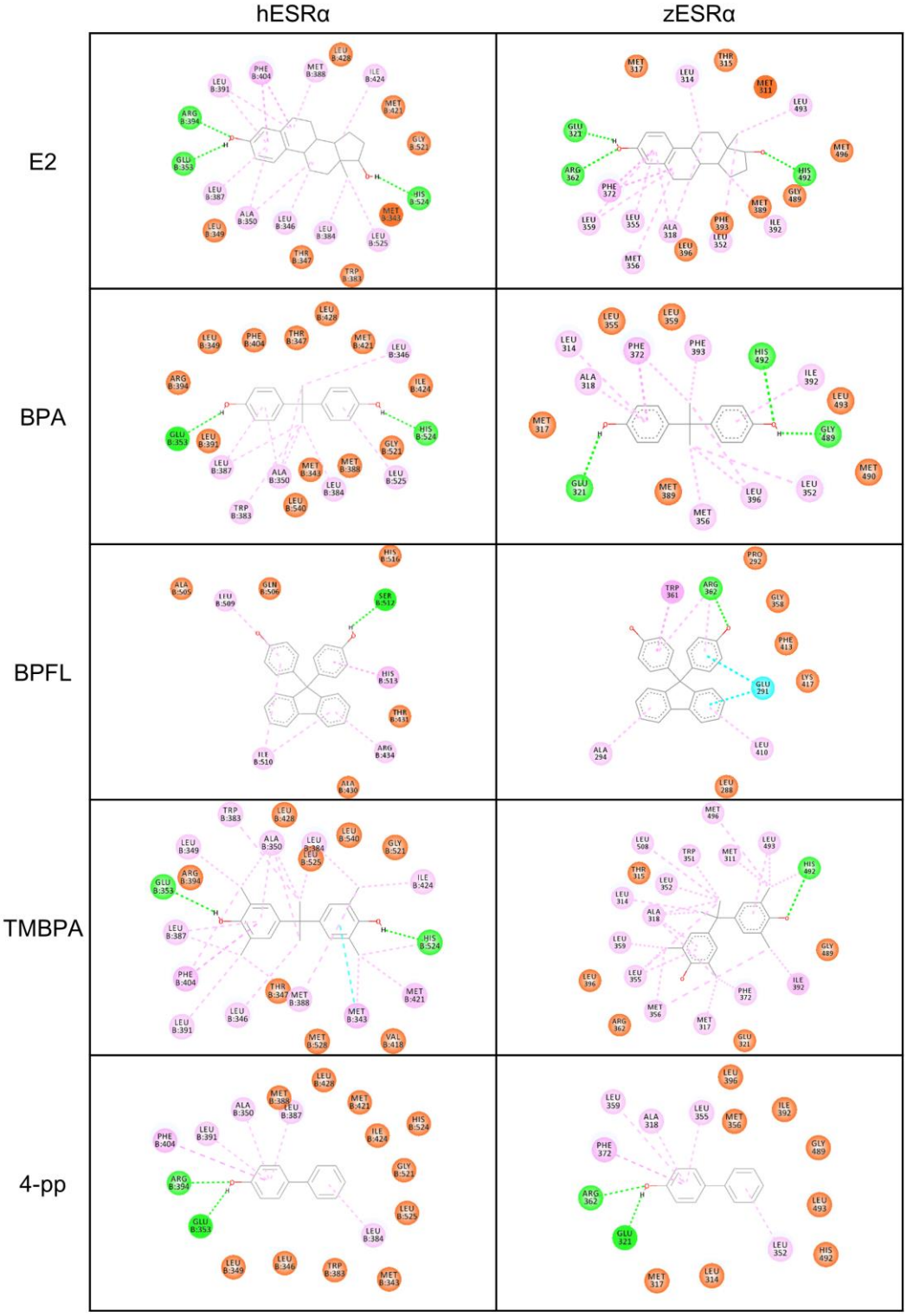

Figure 3. Interactions of the ligand-receptor complexes. 2D docking results for receptor-ligand complex indicating hydrogen bonding (green), hydrophobic

interactions (pink), van der Waals interactions (orange), and electrostatic interactions (cyan).

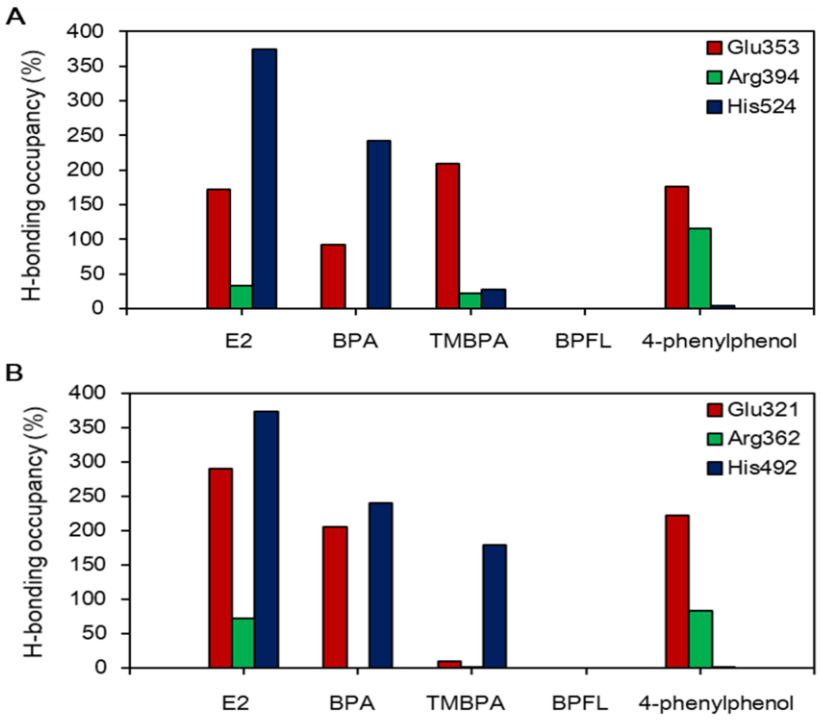

Figure 4. Occupancies of hydrogen bonds between ligands and Glu353, Arg394, and His524 residues for ligand-binding domain of human estrogen receptor 1 (hESR1-

LBD) (A), and between ligands and Glu321, Arg362, and His492 residues for ligand-binding domain of zebrafish estrogen receptor 1 (zEsr1-LBD) (B) during MD simulations (10–15 ns).

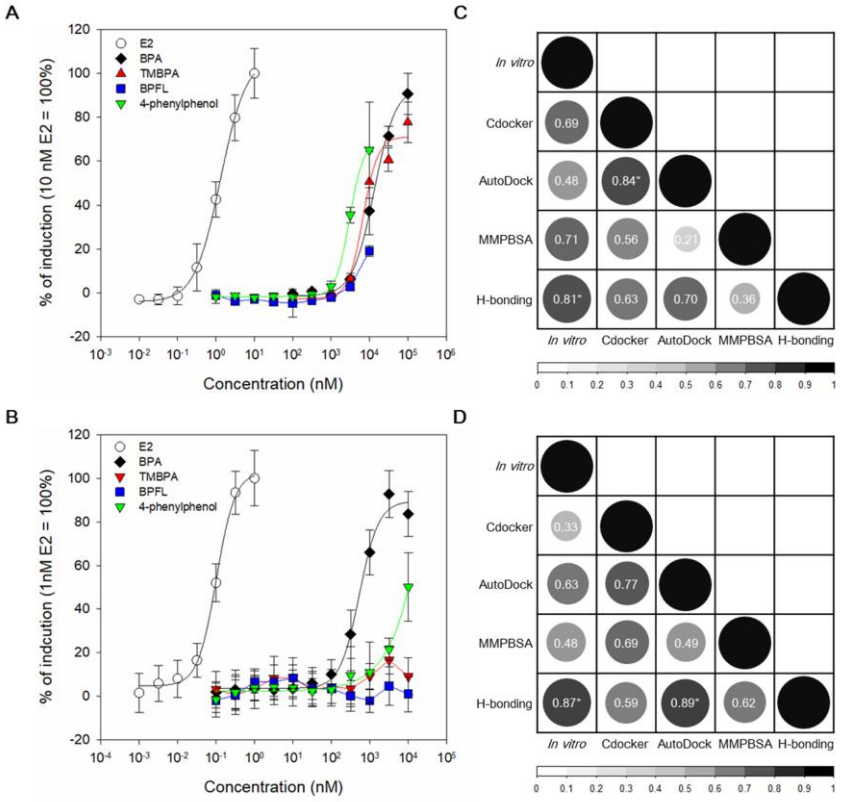

Figure 5. Comparisons of in silico and in vitro assays. (A–B) In vitro assays for estrogenic activity in hESR1 (A) and zEsr1 (B), respectively. The induction value at the maximum concentration of 17β-estradiol (E2; 10 nM for hESR1 and 1 nM for zEsr1) was set to 100%. (C-D) Correlation matrix plot. Pearson correlation coefficient (r) between in silico and in vitro results in hESR1 (C) and zEsr1 (D), respectively. Values are indicated as r2. The color intensity and the size of rounds are proportional to r2. An asterisk indicates significant correlation ($p < 0.05$). The applied in vitro data are the maximal induction ratios of each chemical. The binding energies computed by Discovery studio, Autodock Vina, and MMBPSA, were applied in the analysis. The H-bonding data are the sum of H-bonding occupancies of each complex during MD simulations.

Table 1. Binding energies of molecular dockings and MD simulation

Docking program	Molecular docking				MD simulation (10 – 15 ns)	
	Discovery Studio Cdocker interaction energy (kcal/mol)		AutoDock Vina Binding free energy (kcal/mol)		MMPBSA Binding free energy, ΔG_{bind} (kcal/mol)	
Ligands/receptors	hESR1-LBD	zEsr1-LBD	hESR1-LBD	zEsr1-LBD	hESR1-LBD	zEsr1-LBD
Estradiol (E2)	-53.2 ± 0.00	-49.8 ± 0.00	-11.1 ± 0.00	-10.7 ± 0.00	-18.8 ± 2.76	-18.6 ± 2.55
Bisphenol A (BPA)	-38.2 ± 0.00	-38.0 ± 0.00	-8.13 ± 0.10	-8.36 ± 0.04	-17.8 ± 3.09	-17.3 ± 3.17
Bisphenol FL (BPFL)	-14.5 ± 0.00	-12.3 ± 0.00	-7.26 ± 0.05	-7.02 ± 0.12	-7.23 ± 2.61	-3.48 ± 4.67
Tetramethyl Bisphenol A (TMBPA)	-41.8 ± 0.00	-42.3 ± 0.00	-8.10 ± 0.08	-8.13 ± 0.12	-22.9 ± 3.46	-16.8 ± 3.79
4-phenylphenol	-30.4 ± 0.00	-29.7 ± 0.00	-7.80 ± 0.00	-7.60 ± 0.00	-13.1 ± 2.64	-12.3 ± 3.53